

CONTINUOUS CASTING OF FIBERS AND WIRES BY  
IN-ROTATING-LIQUID SPINNING

Georg Frommeyer, Bernhard Heyder and Andreas Ludwig

Max-Planck-Institut für Eisenforschung GmbH  
Department of Materials Science and Technology  
Postfach 140444  
4000 Düsseldorf, Germany

Abstract

Fibers, 100 to 300 microns in diameter, of Sn, Al, Cu, FeSi, FeSiB, and Ni<sub>3</sub>Al alloys were continuously cast by rapidly quenching a jet of liquid metal into a rotating water bath. In-rotating-liquid spinning enables the production of fibers with a small variation in diameter ( $\leq \pm 5\%$ ), several hundred meters in length. The cooling rate of the fibers was estimated to be on the order of  $4 \times 10^4$  K/s. A correlation was established between the physical properties of the molten metal, such as density, viscosity, and surface tension, and the process parameters, e.g. crucible pressure, jet length, injection angle into the coolant, and drum rotational frequency. In addition to optimization of the process parameters, the microstructure and mechanical properties of fibers from diverse materials were investigated.

presented at the symposium  
'Melt-spinning and Strip Casting'  
on the TMS Annual Meeting  
San Diego, march 1992

## Introduction

Compared with conventional wire drawing, there are many advantages to cast wires and fibers directly in diameters smaller than those of wire rods with cross sections close to final dimension. Rolling mills with specific profiles are no longer needed, nor is any elaborate intermediate annealing to reduce strain hardening. For final treatment it is possible to finish-draw the directly cast wire in few passes to obtain a specific surface quality or a preferred microstructure, e.g. to improve the strength properties. The microstructural inhomogeneities caused by low solidification rates and the defects produced by rolling and/or drawing do not occur.

The ejection of molten material through a round nozzle with several tens or hundreds of micrometers in diameter and the subsequent solidification is applied in the production of polyamide fibers (e.g. nylon and perlon). Metal fibers, however, owing to the different physical properties in the molten state, are incomparably more difficult to produce than polyamide or glass fibers, although the first patent for the direct casting of metal fibers were registered back in 1882 [1]. Fibers can be drawn out of a high-viscous melt very easily due to the high drip forming time. A free jet of a low-viscous melt, on the other hand, will break up after a three orders of magnitude smaller time interval (Table 1).

The continuous liquid stream which emerges from a nozzle has no solid boundary. This free jet is in an unstable equilibrium state governed by forces of viscosity, surface tension and inertia. Disturbances of a particular wave length on the jet surface will lead after a certain time to the break up of the jet. Viscous media such as polyamide solidify through air cooling before necking of the jet occurs. With materials such as metallic melts, on the other hand, the viscosity is several orders of magnitude lower. Consequently, the jet breaks after a few milliseconds before solidification takes place (Table 1).

Physical data Material	Melting temperature $T_m$ [°C]	Surface tension $\sigma$ [N/m]	Dynamic viscosity $\eta$ [Pa·s]	drip forming time [s]
Glass (Duran)	1270*	$3.6 \cdot 10^{-1}$	$1 \cdot 10^3$	3
Quartz	1655**	$3 \cdot 10^{-1}$	$4 \cdot 10^6$	> 10
Steel	1500	1.7	$5 \cdot 10^{-3}$	$2 \cdot 10^{-3}$
Aluminium	660	$9.1 \cdot 10^{-1}$	$1.3 \cdot 10^{-1}$	$2.5 \cdot 10^{-3}$
Polyamide	285	$3.6 \cdot 10^{-2}$	$1.4 \cdot 10^2$	2
Water	0	$7.5 \cdot 10^{-2}$	$1 \cdot 10^{-3}$	$2.1 \cdot 10^{-3}$

Table 1: Low viscosity together with high surface tension reduces the stability of a free metal jet as compared with high-viscous melts e.g. of glass or polyamide (\* processing temperature, \*\* softening temperature)

Metal fibers can still be produced from a free melt jet despite this drawback in one of two ways:

- Formation of a viscous boundary layer consisting of high-melting oxides, nitrides etc. to

delay the collapse of the free jet before for solidification takes place.

- Solidification through intensified extraction of heat during the collapsing period.

Both approaches have been pursued. Taylor [2] used in 1924 a layer of viscous glass to produce thin fibers. At the end of the 1970s, American and French companies [3,4] attempted to stabilize the jet with an appropriate combination of alloy and reactive atmosphere. A stabilizing layer of this type must, however, fulfil a number of restrictive requirements:

- a higher melting point than that of the initial melt,
- low solubility in the melt,
- the reactant must be thermodynamically stable in relation to the melt,
- the surface oxidation must take place at high formation rate,
- the layer must be sufficiently thick,
- the layer should be removable or it must not impair the fiber's service properties.

In the second approach, the jet is injected into a coolant. The solidification occurs with high quenching rate before the hydromechanical instability causes the jet to break. This was the idea behind experiments in which the metal jet was injected into a water-filled container or in a tube with through-flowing water stream [5,6]. At the beginning of the 1980s a process called in-rotating-liquid spinning based on this technique was then patented by Ohnaka [7].

#### Experimental procedure

In the in-rotating-liquid spinning process, low superheated molten metal is accelerated by pressure of inert gas through a fine round nozzle, 100- 300  $\mu\text{m}$  in diameter. The melt leaves the nozzle as a free metal jet at velocities of between 5 and 15 m/s. After a free flight distance of a few millimeters, the jet dives into the rotating cooling medium. This process is

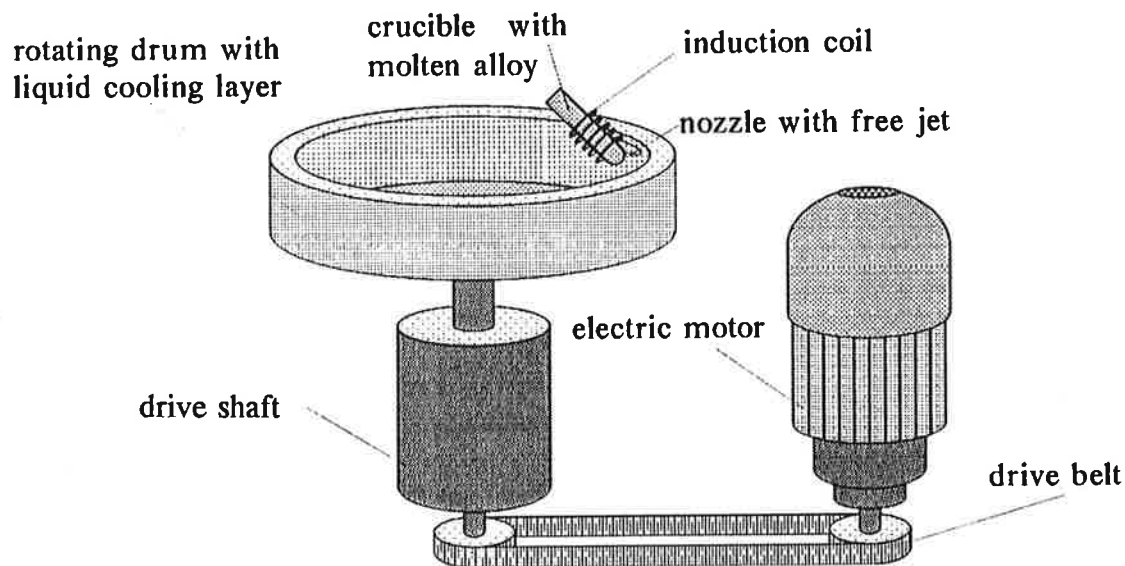


Fig.1. Schematic drawing of the in-rotating-liquid spinning equipment set-up. The casting drum is horizontally attached to the drive shaft. The free jet emerging from the nozzle is quenched and conveyed by the rotating coolant.

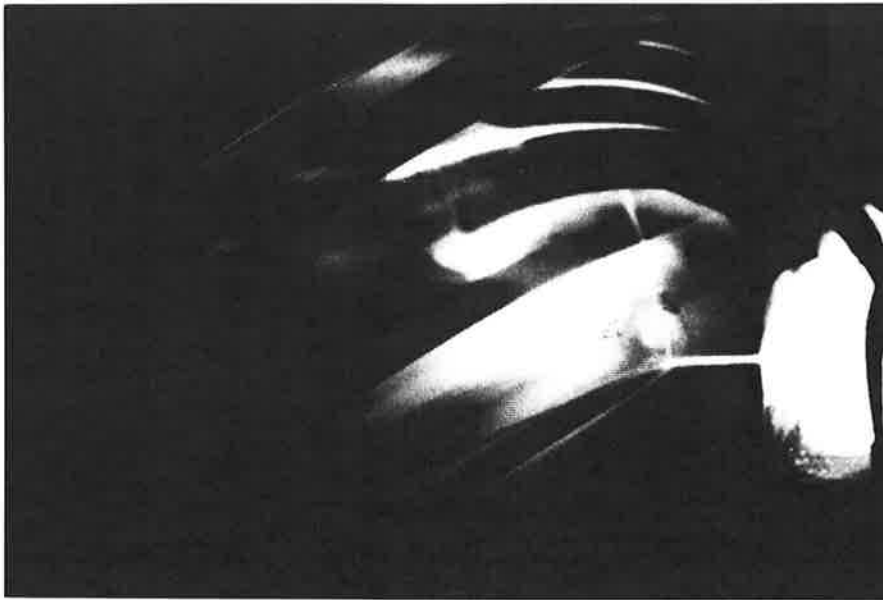


Fig.2. Image of a metallic free jet emerging the nozzle and immersing in the coolant.

characterized by a high stability independent of the jet velocity. An evaluation of the grain size of  $\text{Fe}_{90}\text{Si}_{10}$  fibers reveals that quenching rates on the order of  $4 \times 10^4$  K/s are achieved, depending on the diameter of the jet and on the coolant used [8].

A computer-controlled and instrumented facility for the direct casting of continuous fiber and wire [8,9] by the in-rotating-liquid spinning process has been developed and used for the process studies presented in this paper (Fig. 1). A transparent plexiglass drum is mounted on a vertical precision spindle that guarantees rotation free from vibrations. The vertical position of the drum is in advantage for simply removing the fibers after the casting process.

The alloy is melted inductively under inert gas in a quartz crucible, after which it is pressed through a boron nitride nozzle that has been optimized with regards to its hydromechanical characteristics [10]. Separate heating of the nozzle is provided to compensate the considerable loss of heat by the boundary layer the rotating coolant. The distance between the nozzle tip and the surface of the coolant is adjusted by a stepping motor and the angle of immersion is set by a turntable. The flow behaviour of the metallic free jet (Fig. 2) is examined by high-resolution video cameras. Demineralized water is preferred as coolant, to which surfactants are added to reduce surface tension. Oil emulsions or salt solutions are also included to increase the temperature interval between the boiling and freezing points so as to reduce the amount of film and nucleate boiling. All the relevant process parameters are recorded and evaluated automatically by a data acquisition system.

For the investigation of the influence of the in-rotating-liquid spinning process parameters on the quality of the continuous fibers, studies have been performed by varying the parameters in a certain range using different types of metals and alloys. Pure metal fibers were produced from Sn, Al, Cu. Additional investigation were carried out casting fibers from Fe 6wt. % Si, the amorphous solidifying  $\text{Fe}_{75}\text{Si}_{10}\text{B}_{15}$  and  $\text{Fe}_{40}\text{Ni}_{40}\text{B}_{20}$ , and the intermetallic  $\text{Ni}_3\text{Al}$ .

## Results and Discussion

One of the most important parameter is the velocity of the free melt jet  $V$ . To control this parameter a relation between the extrusion pressure  $\Delta p$  and  $V$  has been derived and compared with experimental data. The flow of the melt at the emergence of the nozzle can be described by the Bernoulli-equation with additional terms considering the nozzle friction  $\Delta p_v$ , the influence of capillarity  $\Delta p_o$ , and the nozzle rejuvenescence friction  $\Delta p_\xi$ . Inserting the different physical properties of metallic melts in the resulting equation reveals that the influence of the surface tension as well as the hydrostatic pressure can be neglected. Thus the modified Bernoulli-equation leads to:

$$\Delta p = \frac{\rho}{2} V^2 + \Delta p_\xi + \Delta p_v = \frac{\rho}{2} V^2 + \frac{\rho}{2} \xi V^2 + \frac{32 \eta l}{\rho d^2} V \quad (1)$$

with  $d$ : diameter of the nozzle,  $l$ : nozzle length,  $\rho$ : density,  $V$ : averaged velocity,  $\xi$ : friction loss factor.

Applying the dimensionless version of eq.1 allows the comparison of different melts. With the definition of the Reynold-number  $Re$  and the pressure coefficient  $c_p$ :

$$Re = \frac{V \cdot d}{2 \eta} \quad c_p = \frac{2 \Delta p}{\rho V^2} \quad (2)$$

eq.1 leads to an equation where only dimensionless quantities are used:

$$c_p \cdot Re^2 = (1 + \xi) Re^2 + 64 \frac{l}{d} Re \quad (3)$$

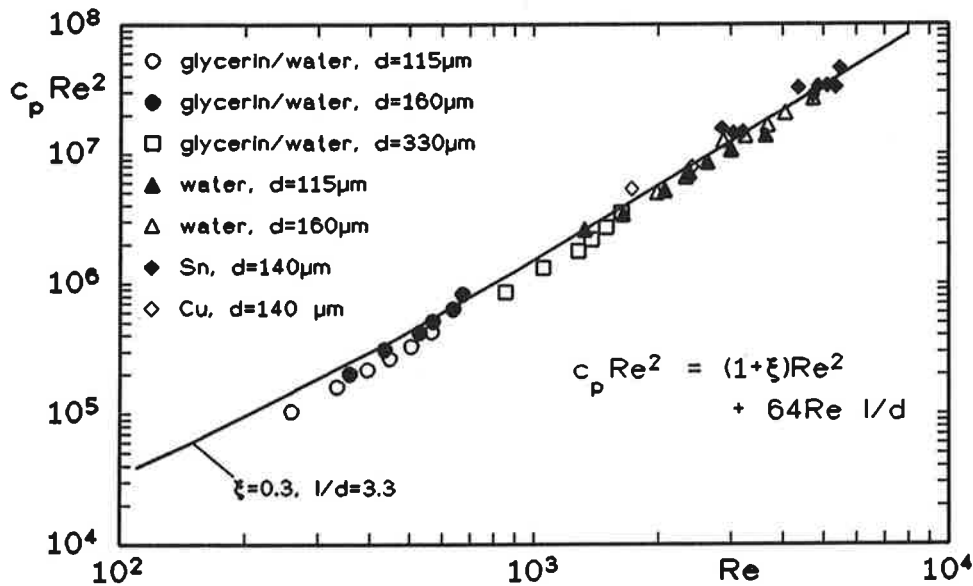


Fig.3. Relation between the dimensionless pressure ( $c_p \cdot Re^2$ ) and the dimensionless flow velocity ( $Re$ ). Using a friction loss factor  $\xi = 0.3$  the experimental data points determined for different melts can be fitted by eq. 3.

The Reynold-number  $Re$  can be interpreted as a dimensionless velocity and  $c_p \cdot Re^2$  as the dimensionless pressure. Fig.3 reveals that the experimentally determined relation between  $Re$  and  $c_p \cdot Re^2$  is valid for different melts and can be well understood by eq.3 using a constant friction loss factor  $\xi = 0.3$ .

For optimising the break-up length, which is a function of jet velocity, different pressures have been applied. The pressure for a metal jet must be set in between 3 and 5 bar to maintain a laminar flow with sufficient stability (Table 2).

Another process parameter of relevance is the superheating of the melt. High solidification rate should be achieved so that the degree of superheating must not be set too high. On the other hand, a low degree of superheating can easily lead to clogging of the nozzle hole. In this case, the heat loss by the circulating air boundary layer at the nozzle orifice causes premature solidification of the melt. In order to prevent this and the oxidation of the melt at the end of the nozzle, additional heating of the nozzle area is provided by a reducing  $H_2$  flame. An optimum interval for the superheat under this conditions was found to be 50 - 100 K.

To ensure the jet solidified before it will break, the distance between the nozzle and the surface of the coolant must be kept on the order of 10 mm. When the liquid free jet impacts on the surface of the coolant, its geometry will only be retained, however, if a solid skin of minimum thickness has already formed, and this takes a certain time. The best fibers can be produce by applying a distance between the nozzle tip and the surface of the coolant of about 5 - 15 mm.

Process parameters	Investigated range	Optimum range
Extrusion pressure [bar]	1.5 - 7	3 - 5
Nozzle diameter [ $\mu\text{m}$ ]	80 - 400	100 - 300
Superheating of melt [ $^{\circ}\text{C}$ ]	50 - 250	50 - 100
Distance between nozzle tip and surface of coolant [mm]	3 - 30	5 - 15
Angle between nozzle and bath [ $^{\circ}\text{C}$ ]	30 - 70	40 - 50
Depth of coolant layer [mm]	5 - 35	15 - 25
Drum speed [rpm]	100 - 220	160 - 200
Drum diameter [mm]	886	
Input weight [g]	30 - 150	

Table 2: Process parameters for in-rotating-liquid spinning (INROLISP)

An acute angle of immersion is favourable for reducing the impact of the melt jet on the cooling medium, but this results in a low quenching rate. There is also the additional risk of bouncing. With steep angles of immersion, on the other hand, the steam bubbles are removed more quickly. This improves the heat transfer but has a negative effect on the geometry of

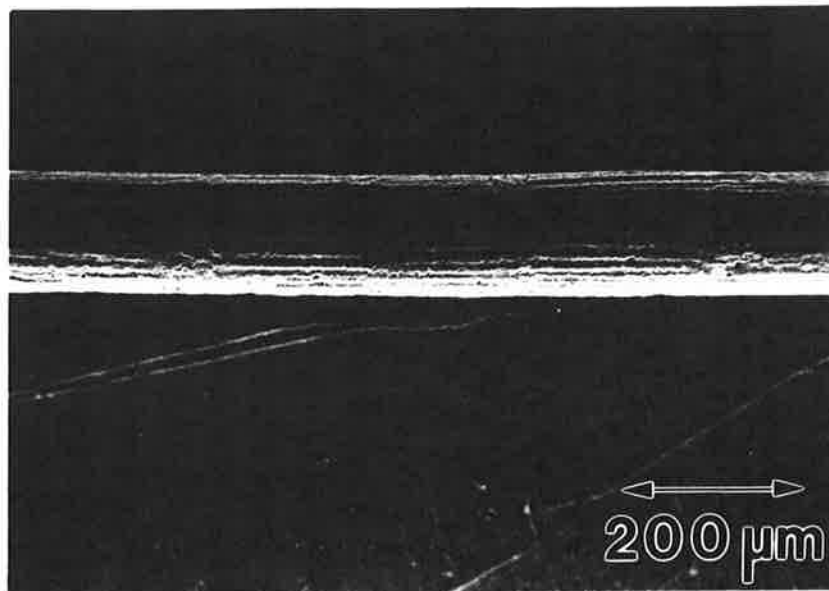


Fig.4. The SEM-image shows the surface topology of a directly cast  $\text{Ni}_3\text{Al}$  fiber. The longitudinal fibrous structure results from the fact that the surface of the wire solidifies at first. During subsequent solidification the cross section of the wire shrinks due to the volumetric decrement.

the fibers. Angles of  $40 - 50^\circ$  were found to result in sufficient fiber quality.

To stabilize the jet as it enters the cooling medium it is necessary to adopt the jet velocity with the tangential velocity of the rotating coolant. The velocity of jet should be marginally higher than that of the coolant surface.

It was found that the diameter of the fibers are slightly smaller than that of the nozzle. The reason for this is the abrupt end of the state of adhesion at the nozzle orifice, causing the velocity profile of the jet to relax into a constant velocity distribution. Very narrow nozzle holes of less than  $50 \mu\text{m}$  in diameter result in clogging from entrained particles of high-melting slag and oxides. Large jet diameters of about  $250 \mu\text{m}$  cause a vigorous film and nucleate pool boiling, which has negative effects on the surface quality of the quenched fiber.

### Conclusions

Because of the high cooling rates of the directly cast fibers, the in-rotating-liquid spinning process falls under the heading of rapid solidification technology. The microstructure of the rapidly solidified fibers exhibits the following advantages:

- segregations are prevented,
- grain sizes are reduced,
- dendrite arm spacings are shortened,
- additional phases are more finely distributed in the microstructure,
- metastable solid-solution supersaturations are produced,
- superlattices can be suppressed,
- production of amorphous fibers is possible.

Thin wires and fibers have great potential applied in composites and as special materials with improved physical and mechanical properties. Amorphous fibers, e.g. FeSiB alloys, display strengths of over 3500 N/mm<sup>2</sup> and can be used as light-weight rope, as wire cord for high-duty tires or as high-strength piano wire. High-melting intermetallic phases such as nickel aluminide (Fig. 4) can be employed as reinforcement fibers in metallic matrix composites with aluminum based alloys. The high solid-solution supersaturation permits production of wire with special magnetical properties. FeSi with more than 6% Si, for example, displays minimum hysteresis loss and so is popular among manufacturers of electrical machines. Shape memory alloys, a much discussed category of late, can also be produced by this process.

In-rotating-liquid spinning is an interesting option for the direct casting of continuous fibers and wires with superior properties. Various producers and users of wires in the U.S.A., France and especially Japan are busy developing the process to production maturity. In addition to controlling jet stability it is still necessary on the equipment side to develop a suitable take-up system and to raise the production rate through parallel operation of several nozzles. Once these problems are solved, the process should find wide acceptance throughout industry.

#### References

1. E. Small, U.S. Patent No. 262 625 (1882)
2. G.F. Taylor, Phys. Review, 23 (1924), 655-660
3. R.E. Cunningham et al., AICHE Symposium Series, 180 (1978), 20-31
4. J.M. Massoubre et al., Revue de Métallurgie 3 (1977), 155-167
5. G.R. Leghorn, U.S. Patent No. 3 430 680 (1969)
6. S. Kavesh, U.S. Patent No. 3 845 805 (1974)
7. I. Ohnaka, Japanese Patent No. 64 948 (1980)
8. B. Heyder and G. Frommeyer, Mat. Sci. Eng. A 133 (1991), 667-670
9. B. Heyder and G. Frommeyer, Wireworld 3 (1991), 20-25
10. B. Heyder, (Ph.D. Thesis, Technical University Aachen, 1992)